

Theoretical Astroparticle Physics

Contents

1	Topics	333
2	Participants	335
2.1	ICRANet participants	335
2.2	Ongoing collaborations	335
3	Brief description	337
3.1	Relativistic kinetic theory and its applications	337
3.2	Electron-positron plasma	337
3.2.1	Relativistic degeneracy in the pair plasma	338
3.2.2	Bose-Einstein condensation in relativistic plasma	340
3.3	Relativistic hydrodynamics	342
3.3.1	On the Role of a Cavity in the Hypernova Ejecta of GRB 190114C	342
3.4	Early Universe	344
3.4.1	Probability of inflation in loop quantum cosmology	344
3.5	Self-gravitating systems of Dark Matter particles	346
3.5.1	Fermionic dark matter in galactic structures	346
4	Publications	353
4.1	Invited talks at international conferences	356
4.2	Lecture courses	356

1 Topics

- Relativistic kinetic theory and its applications
- Electron-positron plasma
 - Thermalization of electron-positron plasma with quantum degeneracy
 - Bose-Einstein condensation in relativistic plasma
- Relativistic hydrodynamics
 - On the Role of a Cavity in the Hypernova Ejecta of GRB 190114C
- Early Universe
 - Probability of inflation in loop quantum cosmology
- Self-gravitating systems of Dark Matter particles
 - Fermionic dark matter galactic structures

2 Participants

2.1 ICRANet participants

- Carlo Luciano Bianco
- Jorge Rueda
- Remo Ruffini
- Gregory Vereshchagin
- She-Sheng Xue

2.2 Ongoing collaborations

- Carlos R. Argüelles (Universidad Nacional de La Plata & CONICET, Argentina)
- Alexey Aksenov (ICAD, RAS, Russia)
- Suzana Bedic (IRAP-PhD, Croatia)
- Stefano Campion (IRAP-PhD, Italy)
- Nikolai Prakapenia (ICRANet-Minsk, Belarus)
- Andreas Krut (ICRANet, Pescara, Italy)
- Julio David Melon Fuksman (IRAP-PhD, Argentina)
- Ivan Siutsou (ICRANet-Minsk, Belarus)
- Rafael Ignacio Yunis (ICRANet, Pescara, Italy)

3 Brief description

Astroparticle physics is a new field of research emerging at the intersection of particle physics, astrophysics and cosmology. Theoretical development in these fields is mainly triggered by the growing amount of experimental data of unprecedented accuracy, coming both from the ground based laboratories and from the dedicated space missions.

3.1 Relativistic kinetic theory and its applications

We pay particular attention to presenting our results in relativistic kinetic theory in a systematic and pedagogic manner. This approach resulted in a lecture course created by G.V. Vereshchagin for the students of the IRAP PhD Erasmus Mundus Joint Doctorate program. In september 2019 lectures were given to the students of the Physics Department of the Belarusian State University.

This lecture course is based on the monograph, co-authored by G.V. Vereshchagin and A.G. Aksenov from ICAD, RAS "Relativistic Kinetic Theory With Applications in Astrophysics and Cosmology", published by Cambridge University Press in 2017 in English and translated in Russian by the leading Russian publishing house "Nauka" in Moscow, with a support by the grant of the Russian Foundation for Basic Research.

3.2 Electron-positron plasma

Electron-positron plasma is of interest in many fields of physics and astrophysics, e.g. in the early universe, active galactic nuclei, the center of our Galaxy, compact astrophysical objects such as hypothetical quark stars, neutron stars and gamma-ray bursts sources. It is also relevant for the physics of ultraintense lasers and thermonuclear reactions. We study physical properties of dense and hot electron-positron plasmas. In particular, we are in-

interested in the issues of its creation and relaxation, its kinetic properties and hydrodynamic description, baryon loading and radiation from such plasmas.

Two different states exist for electron-positron plasma: optically thin and optically thick. Optically thin pair plasma may exist in active galactic nuclei and in X-ray binaries. The theory of relativistic optically thin nonmagnetic plasma and especially its equilibrium configurations was established in the 80s by Svensson, Lightman, Gould and others. It was shown that relaxation of the plasma to some equilibrium state is determined by a dominant reaction, e.g. Compton scattering or bremsstrahlung.

Developments in the theory of gamma ray bursts from one side, and observational data from the other side, unambiguously point out on existence of optically thick pair dominated non-steady phase in the beginning of formation of GRBs. The spectrum of radiation from optically thick plasma is usually assumed to be thermal.

In a series of publications we consider kinetic, electrodynamic, hydrodynamic and observational properties of relativistic plasma.

3.2.1 Relativistic degeneracy in the pair plasma

It is well known that at relativistic temperatures plasma becomes degenerate. In order to study relativistic degeneracy we have introduced the Bose enhancement and Pauli blocking factors in the Boltzmann equations that allows us to follow the relaxation of the pair plasma to Planck spectrum of photons and Fermi-Dirac distribution of electrons and positrons. This improvement allows us to study higher energy densities with respect to those treated before. However, for such high energy densities the assumption adopted in these works, namely that three-particle interactions operate on longer timescale with respect to two-particle ones, does not hold. For this reason we had to introduce the collisional integrals for three-particle interactions based on the exact QED matrix elements, in full analogy with previously treated two-particle interactions. In doing this numerical scheme had to be revised and various technical improvements were introduced allowing to perform 12-dimensional integrals in a reasonable time from the computational viewpoint.

This year we considered relaxation of nonequilibrium optically thick pair plasma to complete thermal equilibrium by integrating numerically relativistic Boltzmann equations with collisional integrals computed from the first

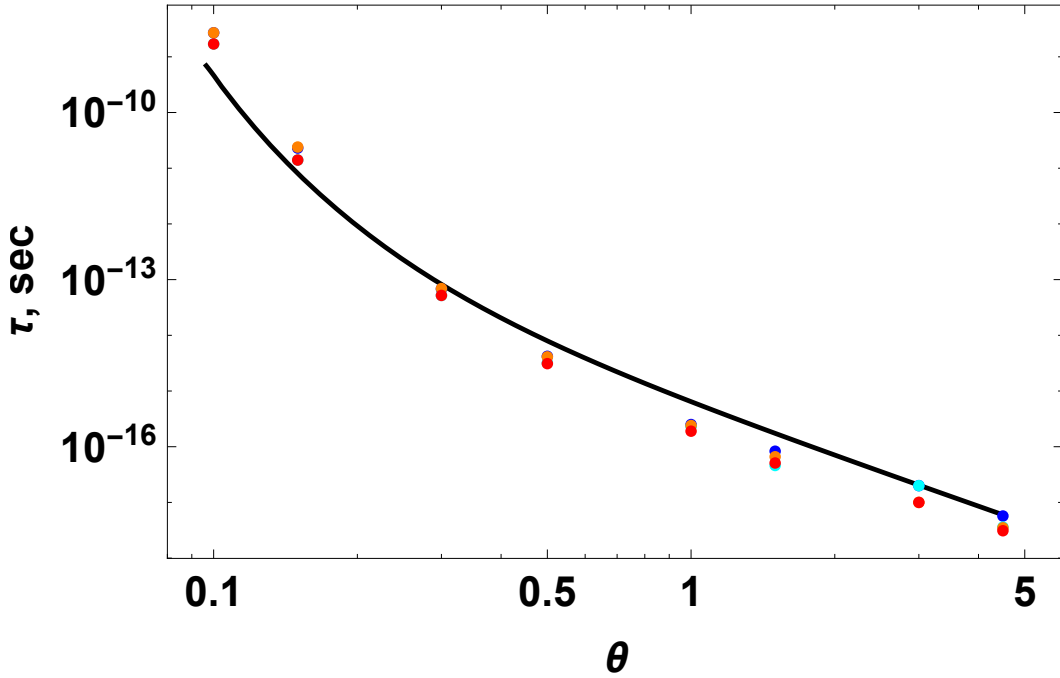


Figure 3.1: Thermalization timescales for electron-positron-photon plasma as a function of the final temperature. Classical statistics with initial pairless state (blue), quantum statistics with initial pairless state (cyan), classical statistics with initial photonless state (orange), quantum statistics with initial photonless state (red). Black curve represents estimated timescales τ_{3p} .

principles, namely from the QED matrix elements both for two-particle and three-particle interactions. We pointed out that unlike classical Boltzmann equation for binary interactions such as scattering, more general interactions are typically described by four collisional integrals for each particle that appears both among incoming and outgoing particles.

Our numerical results indicate that the rates of three-particle interactions become comparable to those of two-particle ones for temperatures T about $k_B T > 0.3m_e c^2$, where k_B is Boltzmann's constant, m_e is electron mass and c is the speed of light. Thus three particle interactions such as relativistic bremsstrahlung, double Compton scattering and radiative pair creation become essential not only for establishment of thermal equilibrium, but also for correct evaluation of interaction rates, energy losses etc.

We developed a new efficient method to compute Uehling-Uhlenbeck collision integral for all two-particle interactions in relativistic plasma with drastic improvement in computation time with respect to existing methods. Plasma is assumed isotropic in momentum space. The set of reactions consists of: Moeller and Bhabha scattering, Compton scattering, two-photon pair annihilation, and two-photon pair production, which are described by QED matrix elements. In our method exact energy and particle number conservation laws are satisfied. Reaction rates are compared, where possible, with the corresponding analytical expressions and convergence of numerical rates is demonstrated.

Collision integrals for all binary and triple reactions were computed from the first principles. Thermalization timescales in the final temperature range $0.1 \leq \theta_{fin} \leq 4.5$ are determined, see Fig. 3.1. We also showed that kinetic equilibrium is absent in relativistic case with final temperature $k_B T > 0.3m_e c^2$. We also found that quantum degeneracy leads to enhanced pair production in initially pairless state.

Results of this work were reported at the 3rd Zeldovich meeting in Minsk, Belarus, 2018. These results are published in Physics Letters A, 2019.

3.2.2 Bose-Einstein condensation in relativistic plasma

The phenomenon of Bose-Einstein condensation is traditionally associated with and experimentally verified for low temperatures: either of nano-Kelvin scale for alkali atoms or room temperatures for quasi-particles or photons in two dimensions. In this work we demonstrate out of first principles that for certain initial conditions non-equilibrium plasma at relativistic temperatures of billions of Kelvin undergoes condensation, predicted by Zeldovich and Levich in their seminal work. It is found that condensation of photons may occur both in nonrelativistic and in relativistic cases and it manifests in photon spectra described by the Planck law with an excess formed in the energy range above the critical energy for the dominance of triple interactions and below the peak of the spectrum. At nonrelativistic temperatures it is well described by a power law, see Fig. 3.2, while at relativistic temperatures it represents a bump. In our nonrelativistic example the condensation persists until about 10^{-8} sec, when complete thermal equilibrium is established.

It is found that necessary condition for the development of BEC is an excess of photon number over the equilibrium number, as well as initial distribution

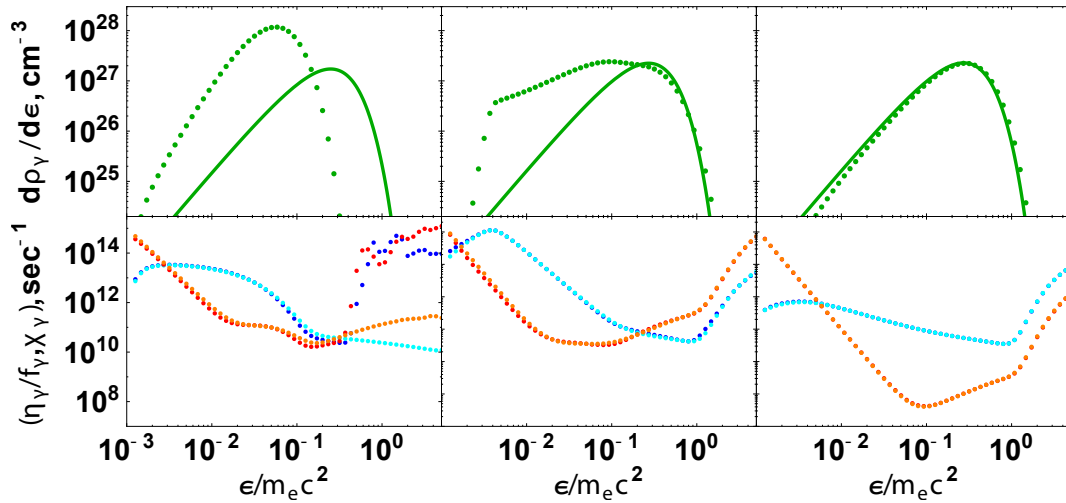


Figure 3.2: Top: The spectral energy density (dots) with the associated Planck fit (solid) for selected time moments from left to right: 10^{-15} , 10^{-11} , 10^{-8} sec, in nonrelativistic case. Bottom: emission and absorption coefficients for photons (binary reactions: emission (blue) and absorption (cyan); triple reactions: emission (purple) and absorption (red)). The left panel represents initial distribution of photons; the middle one shows photon condensation, while the right one corresponds to the final state.

of photons not broader than Wien spectrum with the peak of the distribution located above the critical energy below which triple interactions dominate over the binary ones. Broader initial distributions, even the Planck spectrum, contain too many photons at low energies, and triple interactions such as bremsstrahlung quickly eliminate excess photons, preventing the condensation. This is the reason why the cooling of photons by electrons proposed by Zeldovich and Levich does not lead to photon condensation.

The results of this work were presented at the 16th Italian-Korean Symposium on Relativistic Astrophysics, July 1-5, 2019, ICRANet, Pescara (Italy) and submitted for publication in European Physics Letters.

3.3 Relativistic hydrodynamics

This year we returned to the research topic of relativistic hydrodynamics of electron-positron-photon plasma on which the group was focused during the last 20 years [Ruffini et al., *A&A* 350 (1999) 334; 359 (2000) 855; *ApJ* 869 (2018) 151; *Il Nuovo Cimento C* 36 (2013) 255].

With the goal of interpretation of the light curve of gamma-ray burst GRB190114C within the binary-driven hypernova I (BdHN I) scenario, the process of hydrodynamic interaction between expanding supernova ejecta and electron-positron plasma created around just formed black hole is considered. The publicly available PLUTO code is used, which implements shock-capturing relativistic hydrodynamics (RHD) and is suitable to perform multidimensional tasks. It is assumed that black hole formation producing a GRB occurs in an extremely tight binary system with a massive CO core, which explodes as a supernova, and a companion neutron star, which after an episode of hypercritical accretion undergoes gravitational collapse. The first spike (Episode 2) originates from electron-positron-photon plasma formed around the black hole, while the second spike (Episode 3) originates from the reflection wave produced by the impact of the plasma on the supernova ejecta. Relativistic hydrodynamic simulations are performed in two dimensions.

3.3.1 On the Role of a Cavity in the Hypernova Ejecta of GRB 190114C

The BdHN I scenario considers a binary system composed of a massive carbon-oxygen core (CO_{core}), and a binary neutron star (NS) companion with a typical binary period of few minutes. It is assumed that at a certain moment the CO_{core} undergoes a supernova explosion with the creation of a new neutron star (νNS). At the same time hypercritical accretion onto the companion binary neutron star initiates and proceeds until it exceeds the critical mass for gravitational collapse. The formation of a black hole (BH) captures 10^{57} baryons by enclosing them within its horizon, and thus a cavity of approximately 10^{11} cm is formed around it with initial density 10^{-7} g/cm³. A further depletion of baryons in the cavity originates from the expansion of the electron-positron-photon ($e^+e^-\gamma$) plasma formed at the collapse, reaching a density of 10^{-14} g/cm³ by the end of the interaction, see Fig. 3.3. It is demon-

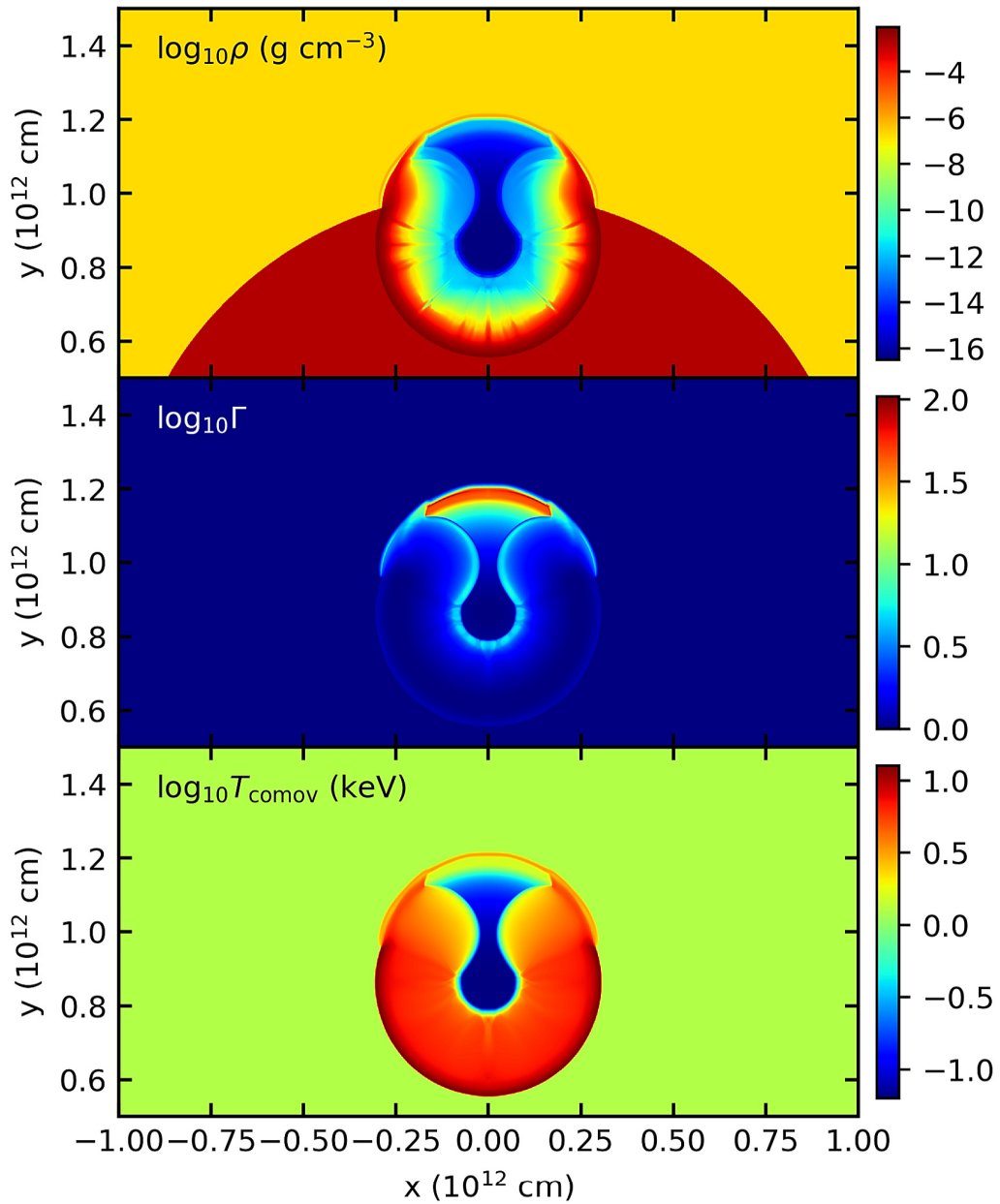


Figure 3.3: Spatial distributions of matter density (top), Lorentz factor (middle) and comoving temperature (bottom) at $t = 11$ s, showing the mildly relativistic reflection wave propagating backward in the cavity, as well as the ultrarelativistic $e^+e^-\gamma$ plasma wave propagating outside the cavity. The shock wave is visible inside the ejecta.

strated here using an analytical model complemented by a hydrodynamical numerical simulation that part of the $e^+e^-\gamma$ plasma is reflected off the walls of the cavity. The consequent outflow and its observed properties are shown to coincide with the featureless emission occurring in a time interval of duration t_{rf} , measured in the rest frame of the source, between 11 and 20 s of the GBM observation. Moreover, similar features of the GRB light curve were previously observed in GRB 090926A and GRB 130427A, all belonging to the BdHN I class. This interpretation supports the general conceptual framework presented in (Ruffini et al., 2019) and guarantees that a low baryon density is reached in the cavity, a necessary condition for the operation of the “inner engine” of the GRB presented in an accompanying article.

The results of this work were presented at the meeting “Supernovae, Hypernovae and Binary Driven Hypernovae, An Adriatic Workshop” held on June 20-30, 2016 in Pescara, Italy. The results of this work are published in ApJ (2019).

3.4 Early Universe

The physics of the early Universe including the issue of initial conditions is an active field of research where participants of the group have contributed. Among the topics considered are: cosmological singularity and bouncing cosmologies, inflationary cosmology and initial conditions for inflation.

Being motivated by the famous work of Belinski, Grishchuk, Khalatnikov and Zeldovich, Phys. Lett. B 155, 232 (1985) on initial conditions for inflation, a number of papers was published, including the well know study of the problem in Loop Quantum Cosmology, by P. Singh, K. Vandersloot, and G. V. Vereshchagin, Phys. Rev. D 74, 043510 (2006).

3.4.1 Probability of inflation in loop quantum cosmology

The issue of initial conditions for cosmological evolution in loop quantum cosmology with attracts a lot of attention, see e.g. Ashtekar and Sloan, Phys. Lett. B 694, 108 (2010). We focused in the simplest case with massive scalar field. It was discussed how the presence of the bounce, which is the specific feature of LQC, influences the probability of inflation in this theory, compared with General Relativity. The main finding is the existence of an attractor in the contracting phase of the Universe, which results in a special probability

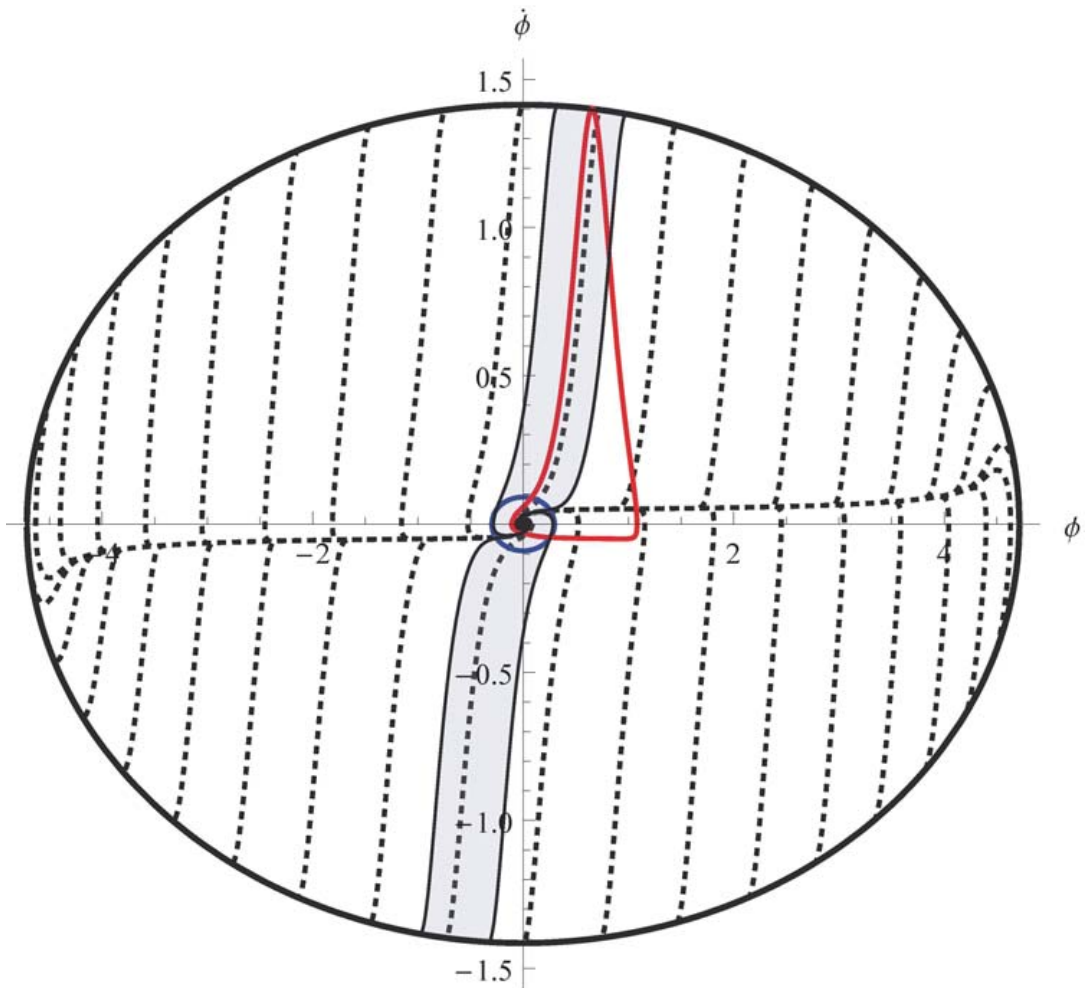


Figure 3.4: Solutions of the cosmological equations of LQC in the $\phi - \dot{\phi}$ diagram. All solutions start in the distant past in the origin, pass through oscillatory phase with increasing amplitude of oscillations and end up at the bounce shown by the thick external circle. Blue internal circle (obtained setting $H = m$) represents the region where most solutions deviate from the repulsive separatrix (located along the horizontal axis, at which the Hubble parameter is nearly constant). This region shrinks with decreasing mass (the value of the mass in this figure is $m = 0.1M_{\text{Pl}}$ selected for better clarity). The red curve shows the complete most probable solution originating from the remote past (including both contraction and expansion phases). This solution has no exponential contraction phase, but it has a successful inflationary phase.

distribution at the bounce, quite independent of the measure of initial conditions in the remote past, and hence a very specific duration of the inflationary stage with the number of e-foldings about 140. The red curve in Fig. 3.4 shows the most probable solution in LQC, presented at the $\phi - \dot{\phi}$ diagram, originating from the remote past, possessing oscillations at the contraction phase, then passing through a regular bounce and successful inflation, eventually ending up with damped oscillations corresponding to reheating. The results of this work are published in *Phys. Rev. D*, 2019.

3.5 Self-gravitating systems of Dark Matter particles

3.5.1 Fermionic dark matter in galactic structures

The problem of the distribution of stars in globular clusters, and more general in galactic systems, has implied one of the results of most profound interest in classical astronomy. Since the pioneering works of Michie [*MNRAS*, 125, p. 127 (1963)] and King [*AJ*, 71, p. 64 (1966)], they considered the effects of collisional relaxation and tidal cutoff by studying solutions of the Fokker-Planck equation. There, it was shown that stationary solutions of this kind can be well described by lowered isothermal spheres models, based on simple Maxwellian energy distributions with a constant subtracting term interpreted as an energy cutoff. An extension of this statistical analysis with thermodynamic considerations, which includes the effects of violent (collisionless) relaxation, has been studied by D. Lynden-Bell in [*MNRAS*, 136, p. 101 (1967)], with important implications to the problem of virialization in galaxies which are still of actual interest. Later on, in a series of works by R. Ruffini et al. (e.g. [*A&A*, 119, p. 35 (1983)] in Newtonian gravity and [*A&A*, 235, p. 1 (1990)] in GR), the emphasis changed from self-gravitating systems of classic stars (which verify Maxwellian distributions) to systems of fermionic particles, with the aim of describing galactic DM halos. It was there considered a quantum fermionic distribution taking into account the possible presence of a cutoff in the energy as well as in the angular momentum. A remarkable contribution in the understanding of these issues was given by P.-H. Chavanis [*Physica A*, 332, p. 89 (2004)], based on the study of generalized kinetic theories accounting for collisionless relaxation processes, and leading to a class

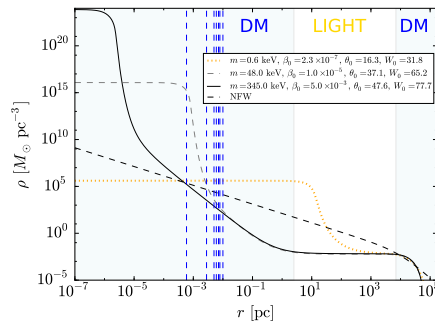


Figure 3.5: (Color online) Theoretical density profiles from 10^{-7} pc all the way to 10^5 pc, for three representative fermion masses in the $mc^2 \sim \text{keV}$ region: 0.6 keV (dotted yellow curve), 48 keV (long-dashed gray curve) and 345 keV (solid black curve). The dashed blue lines indicate the position of the S-cluster stars by Gillessen et al. [ApJ, 707, p. L114 (2009)]. We show for the sake of comparison the NFW density profile as obtained by Sofue in [PASJ, 65, p. 118 (2013)] (dashed black curve). See [IJMPD, 28, i. 14 (2019)] for additional details.

of generalized Fokker-Planck equation for fermions. It was there explicitly shown the possibility to obtain, out of general thermodynamic principles, a generalized Fermi-Dirac distribution function including an energy cutoff, extending the former results by Michie and King to quantum particles. More recently, it was shown that quantum particles fulfilling fermionic quantum statistics and gravitational interactions are able to successfully describe the distribution of galactic DM halos when contrasted with observations.

This was done through the development of a new model for the distribution of DM in galaxies, the Ruffini-Argüelles-Rueda (RAR) model [MNRAS, 451, p. 628 (2015)], based on a self-gravitating system of massive fermions at finite temperatures, and its recent extension including for escape of particle effects [PDU, 21, p. 82 (2018)]. The RAR model, for fermion masses in the range $\sim 10 - 100$ keV, successfully describes the DM halo in the Galaxy, and predicts the existence of a denser quantum core towards its centre which works as an alternative to the massive Black Hole in SgrA*. This year, the authors have extended the application of the RAR theory to different galactic structures, from dwarf, all the way to galaxy clusters, while discussing the potential consequences in cosmology. The results were published in [PDU, 24, p. 278 (2019)] (see below), including the third winner prize by the Gravity

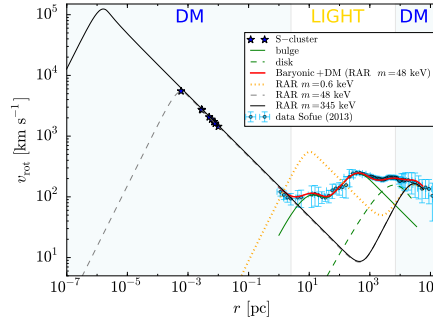


Figure 3.6: (Color online) Theoretical RAR rotation curves from 10^{-7} pc all the way to 10^5 pc, for three representative fermion masses in the $mc^2 \sim \text{keV}$ region: 0.6 keV (dotted yellow curve), 48 keV (long-dashed gray curve) and 345 keV (solid black curve). These RAR solutions are in agreement with all the Milky Way observables from $\sim 10^{-3}$ pc to $\sim 10^5$ pc. For the case of $mc^2 = 48$ keV, we include the total rotation curve (red thick curve) including the total baryonic (bulge + disk) component. The star symbols represent the eight best resolved S-cluster stars by Gillessen et al. [ApJ, 707, p. L114 (2009)] in accordance with the above figure. See [IJMPD, 28, i. 14 (2019)] for further details

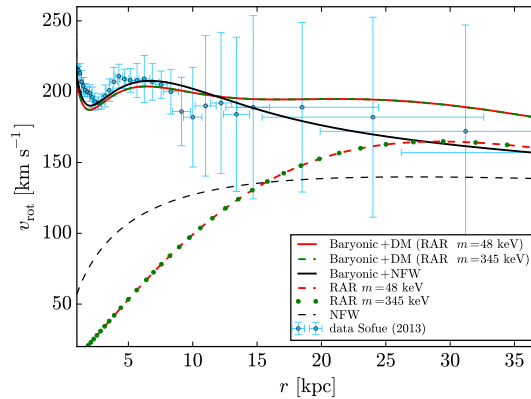


Figure 3.7: (Color online) Comparison of the total (DM plus baryonic) rotation curves as given by the RAR model (for a fermion mass $mc^2 = 48$ keV and 345 keV) and the phenomenological NFW model in the region $r = 1 - 35$ kpc. Within the region 1 – several kpc, the contribution of the baryonic components dominates respect to the DM, while at distances $r \gtrsim 10$ kpc there is, instead, an increasing dominance of the DM component (see [IJMPD, 28, i. 14 (2019)] for further details).

Research Foundation 2019 published in [IJMPD, 28, i. 14 (2019)]. The main results regarding the astrophysical implications on DM halos and predictions of the general RAR theory are:

1. That a regular and continuous distribution of \sim keV fermions can be an alternative to the black hole scenario in SgrA*, being at the same time in agreement with the Milky Way DM halo, and without spoiling the known baryonic (bulge and disk) components which dominate at intermediate scales (See Figs. 3.5, 3.6 and 3.7 for details, the later a zoom-in towards the outer halo region showing a comparison with the NFW fit).
2. By constraining the DM quantum core to have the minimum compactness required by the S2 star dynamics and by requesting the gravitational stability of the entire DM configuration, the fermion mass can be constrained to the range $48 \text{ keV} \lesssim mc^2 \lesssim 345 \text{ keV}$ (See Figs. 3.5 and 3.6 for details).
3. By extending this novel approach to different galaxy types with given halo observables (see Fig. 3.8 for the full family of possible RAR solutions in each galaxy-case), and for fermion masses in the above keV range, the model is shown to be consistent with (a) the observationally inferred correlation between the mass of the dark central object and total DM halo mass by Ferrarese [ApJ, 578, p. 90 (2002)], and with (b) the observationally inferred (universal) value of the inner surface density of DM halos, from dwarf to elliptical, to galaxy clusters by Donato et al. [MNRAS, 397, p. 1169 (2009)]. See Fig. 3.9 and Fig. 3.10 for more details regarding (a) and (b) respectively.

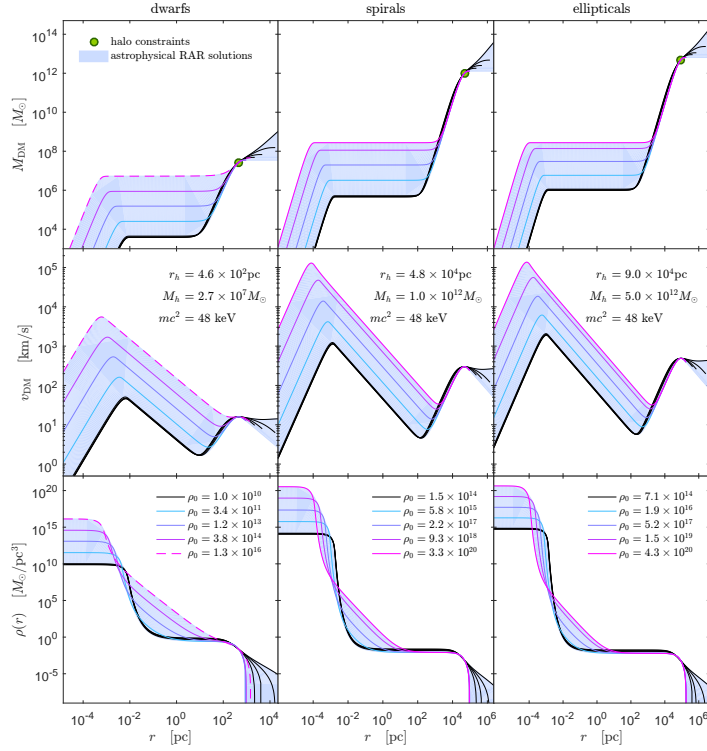


Figure 3.8: (Colour online) Full window of the astrophysical RAR solutions (blue shaded regions enveloped by the 5 benchmark solutions inside), including density profiles (bottom), rotation curves (middle) and DM mass distributions (top); and fulfilling with the observationally given DM halo restriction (r_h, M_h) for typical dwarf (left), spiral (middle) and elliptical galaxies (right), for the relevant case of $mc^2 = 48$ keV. The continuous-magenta curves occurring only for spiral and elliptical galaxies, indicates the critical solutions harboring compact critical cores (before collapsing to a BH) of $M_c^{cr} = 2.2 \times 10^8 M_\odot$, while the dashed-magenta curves for dwarfs are limited (instead) by the astrophysical necessity of a maximum in the halo rotation curve. The bounding black solutions correspond to the ones having the minimum core mass (or minimum ρ_0) which in turn implies the larger cutoff parameters (see Appendix in [PDU, 24, p. 278 (2019)]), thus developing the more extended density tails allowed by the RAR theory, being $\rho \propto r^{-2}$ the limiting isothermal density tail (achieved when $W_0 \rightarrow \infty$).

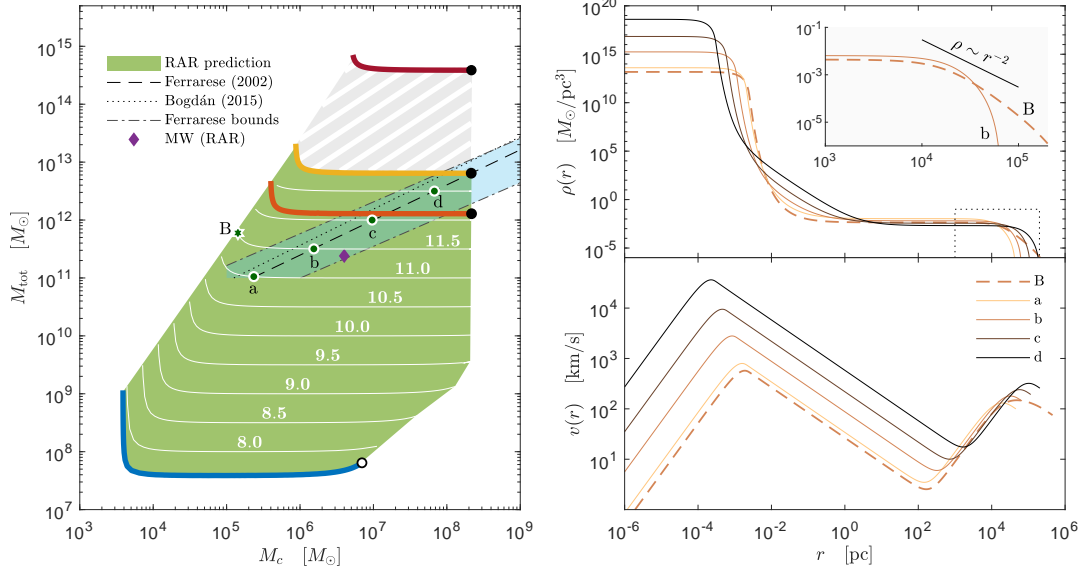


Figure 3.9: (left) Prediction of the $M_c - M_{tot}$ relations within three parametric RAR model (for $mc^2 = 48$ keV). The different coloured lines read for each galaxy type in correspondence with the astrophysical RAR solutions as given in 3.8. The green area, on the other hand, covers all RAR predictions. The white lines show a set of families with given halo mass M_h (and labeled by the M_{tot} value in the horizontal regime). The results show the ability of the RAR model to be in agreement with the different $M_{bh} - M_{tot}$ relations, as considered in the literature, and explicated in the blue-ish stripe. The shaded area above ellipticals is just the extrapolation of the $M_c - M_{tot}$ RAR prediction for BCGs obtained assuming the constant (best fit) of the Donato relation). The filled-black dots correspond to the critical core mass $M_c^{cr} = 2.2 \times 10^8 M_\odot$, and the empty-black dot indicates the limiting maximum core mass for dwarfs. **(right)** Density and velocity profiles associated with the 4 benchmark solutions of the left panel labeled by (a-d). Such solutions lie along the best-fit of Ferrarese with the given mean surface density of about $140 M_\odot / pc^2$. While the dashed curve (B) representing an isothermal-like RAR solution (corresponding with dot B in left-panel) is clearly disfavored by the observed correlation, the continuous curves (as e.g. (b)) are favored. Figure taken from [PDU, 24, p. 278 (2019)]

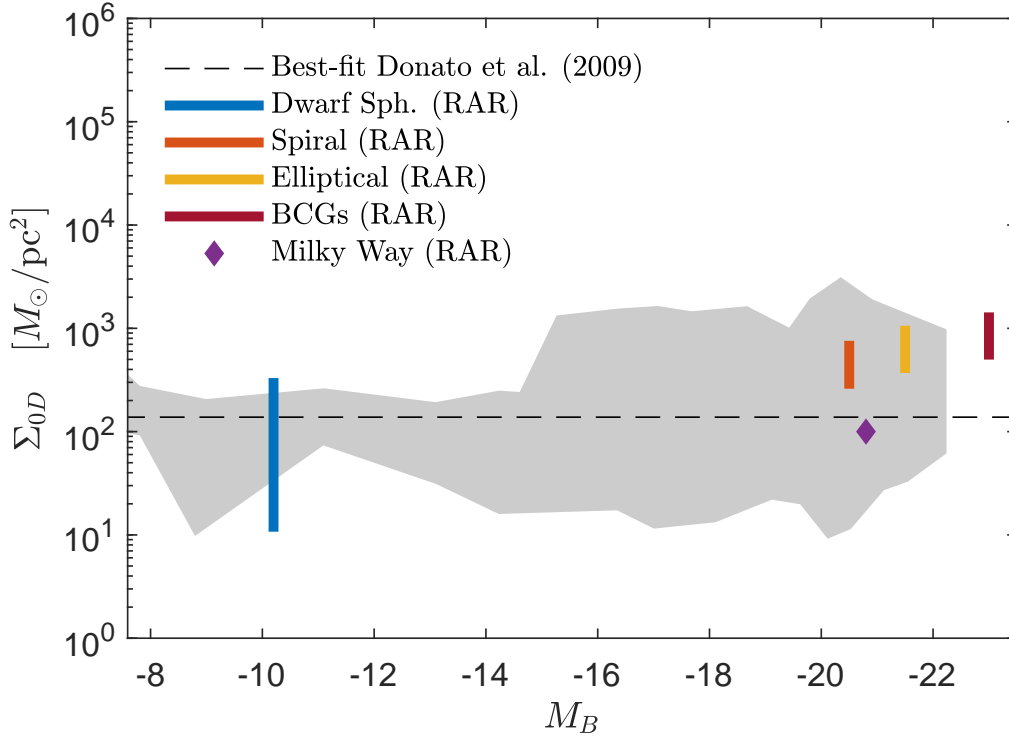


Figure 3.10: The surface DM density as predicted by the RAR model (see vertical colour lines) for each galactic structure in correspondence with the astrophysical solutions (i.e. blue-shaded regions in 3.8). The dashed horizontal line represents the Universal relation from the best fit of the data as found by Donato et al. The dark-gray region indicates the delimited area by the $3 - \sigma$ error bars of all the data points. The result shows the ability of the three parametric RAR model (for $mc^2 = 48$ keV) to be in agreement with the DM surface density observations (see text for further details regarding BCGs).

4 Publications

1. M. A. Prakapenia, I. A. Siutsou and G. V. Vereshchagin, “Thermalization of electron-positron plasma with quantum degeneracy”, *Physics Letters A* 383 (2019) pp. 306-310.

The non-equilibrium electron-positron-photon plasma thermalization process is studied using relativistic Boltzmann solver, taking into account quantum corrections both in non-relativistic and relativistic cases. Collision integrals are computed from exact QED matrix elements for all binary and triple interactions in the plasma. It is shown that in non-relativistic case (temperatures $k_B T \leq 0.3m_e c^2$) binary interaction rates dominate over triple ones, resulting in establishment of the kinetic equilibrium prior to final relaxation towards the thermal equilibrium, in agreement with the previous studies. On the contrary, in relativistic case (final temperatures $k_B T \geq 0.3m_e c^2$) triple interaction rates are fast enough to prevent the establishment of kinetic equilibrium. It is shown that thermalization process strongly depends on quantum degeneracy in initial state, but does not depend on plasma composition.

2. R. Ruffini, J. D. Melon Fuksman and G. V. Vereshchagin, “On the Role of a Cavity in the Hypernova Ejecta of GRB 190114C”, *The Astrophysical Journal*, Vol. 884, Issue 1 (2019) article id. 191.

Within the binary-driven hypernova I (BdHN I) scenario, the gamma-ray burst GRB190114C originates in a binary system composed of a massive carbon-oxygen core (CO_{core}), and a binary neutron star (NS) companion. As the CO_{core} undergoes a supernova explosion with the creation of a new neutron star (ν NS), hypercritical accretion occurs onto the companion binary neutron star until it exceeds the critical mass for gravitational collapse. The formation of a black hole (BH) captures 10^{57} baryons by enclosing them within its horizon, and thus a cavity of approximately 10^{11} cm is formed around it with initial density 10^{-7} g/cm³. A further depletion of baryons in the cavity originates from the expansion of the electron-positron-photon ($e^+e^-\gamma$) plasma formed at the collapse, reaching a density of 10^{-14} g/cm³ by the end of the interaction. It

is demonstrated here using an analytical model complemented by a hydrodynamical numerical simulation that part of the $e^+e^-\gamma$ plasma is reflected off the walls of the cavity. The consequent outflow and its observed properties are shown to coincide with the featureless emission occurring in a time interval of duration t_{rf} , measured in the rest frame of the source, between 11 and 20 s of the GBM observation. Moreover, similar features of the GRB light curve were previously observed in GRB 090926A and GRB 130427A, all belonging to the BdHN I class. This interpretation supports the general conceptual framework presented in (Ruffini et al., 2019) and guarantees that a low baryon density is reached in the cavity, a necessary condition for the operation of the “inner engine” of the GRB presented in an accompanying article.

3. G.V. Vereshchagin and S. Bedic, “Inflationary measure in loop quantum cosmology”, *Phys. Rev. D* 99 (2019) 043512.

We discuss how initial conditions for cosmological evolution can be defined in Loop Quantum Cosmology with massive scalar field and how the presence of the bounce influences the probability of inflation in this theory, compared with General Relativity. The main finding of the paper is existence of an attractor in the contracting phase of the universe, which results in special probability distribution at the bounce, quite independent on the measure of initial conditions in the remote past, and hence very specific duration of inflationary stage with the number of e-foldings about 140.

4. M. A. Prakapenia and G.V. Vereshchagin, “Bose-Einstein condensation in relativistic plasma”, *European Physics Letters*, submitted.

The phenomenon of Bose-Einstein condensation is traditionally associated with and experimentally verified for low temperatures: either of nano-Kelvin scale for alkali atoms [1-3] or room temperatures for quasi-particles [4,5] or photons in two dimensions [6]. Here we demonstrate out of first principles that for certain initial conditions non-equilibrium plasma at relativistic temperatures of billions of Kelvin undergoes condensation, predicted by Zeldovich and Levich in their seminal work [7]. We determine the necessary conditions for the onset of condensation and discuss the possibilities to observe such a phenomenon in laboratory and astrophysical conditions.

5. C. R. Argüelles, A. Krut, J. A. Rueda, R. Ruffini, “Novel constraints on fermionic dark matter from galactic observables II: Galaxy scaling relations”, *Physics of the Dark Universe*, Volume 24 (2019), article id.

100278.

We have recently introduced in paper I an extension of the Ruffini-Argüelles-Rueda (RAR) model for the distribution of DM in galaxies, by including for escape of particle effects. Being built upon self-gravitating fermions at finite temperatures, the RAR solutions develop a characteristic dense quantum core-diluted halo morphology which, for fermion masses in the range $mc^2 \approx 10 - 345\text{keV}$, was shown to provide good fits to the Milky Way rotation curve. We study here for the first time the applicability of the extended RAR model to other structures from dwarfs to ellipticals to galaxy clusters, pointing out the relevant case of $mc^2 = 48\text{keV}$. By making a full coverage of the remaining free parameters of the theory, and for each galactic structure, we present a complete family of astrophysical RAR profiles which satisfy realistic halo boundary conditions inferred from observations. Each family-set of RAR solutions predicts given windows of total halo masses and central quantum-core masses, the latter opening the interesting possibility to interpret them as alternatives either to intermediate-mass BHs (for dwarf galaxies), or to supermassive BHs (SMBHs, in the case of larger galaxy types). The model is shown to be in good agreement with different observationally inferred scaling relations such as: (1) the Ferrarese relation connecting DM halos with supermassive dark central objects; and (2) the nearly constant DM surface density of galaxies. Finally, the theory provides a natural mechanism for the formation of SMBHs of few $10^8 M_\odot$ via the gravitational collapse of unstable DM quantum-cores.

6. C. R. Argüelles, A. Krut, J. A. Rueda, R. Ruffini, "Can fermionic dark matter mimic supermassive black holes? ", *International Journal of Modern Physics D* Vol. 28, No. 14, 1943003 (2019).

We analyze the intriguing possibility of explaining both dark mass components in a galaxy: the dark matter (DM) halo and the supermassive dark compact object lying at the center, by a unified approach in terms of a quasi-relaxed system of massive, neutral fermions in general relativity. The solutions to the mass distribution of such a model that fulfill realistic halo boundary conditions inferred from observations, develop a high-density core supported by the fermion degeneracy pressure able to mimic massive black holes at the center of galaxies. Remarkably, these dense core-diluted halo configurations can explain the dynamics of the closest stars around Milky Way's center (SgrA*) all the way to the halo rotation curve, without spoiling the baryonic bulge-

disk components, for a narrow particle mass range $mc^2 \sim 10 - 10^2$ keV.

4.1 Invited talks at international conferences

1. "On the role of a cavity in the hypernova ejecta of GRB 190114C", The Open Universe International Doctoral School "The discovery of Black Holes", Villa Ratti, Nice, France, June 10 - 14, 2019.
2. "On Bose-Einstein condensation in relativistic plasma", 16th Italian-Korean Symposium on Relativistic Astrophysics, ICRANet, Pescara, Italy, July 1-5, 2019.
3. "Cavity in the hypernova ejecta of GRB 190114C", 105 Congress of the Italian Physical Society, Gran Sasso Science Institute, L'Aquila, Italy, 23-27 September 2019.

4.2 Lecture courses

1. "Relativistic kinetic theory and its applications in astrophysics and cosmology", 5 lectures
(G.V. Vereshchagin)
Lecture course for the students of the Physics Department of Belarusian State University, Minsk, Belarus, 5 - 15 September, 2019.
2. Public lectures "Contemporary astrophysics and its perspectives in Belarus", Belarusian State University and Minsk Science Club, September 2019.